

*Citation for published version:*

Thomas, T & Bowen, CR 2016, 'Effect of particle size on the formation of  $Ti_3AlC_3$  using combustion synthesis', *Ceramics International*, vol. 42, no. 3, pp. 4150-4157. <https://doi.org/10.1016/j.ceramint.2015.11.088>

*DOI:*

[10.1016/j.ceramint.2015.11.088](https://doi.org/10.1016/j.ceramint.2015.11.088)

*Publication date:*

2016

*Document Version*

Peer reviewed version

[Link to publication](https://doi.org/10.1016/j.ceramint.2015.11.088)

**University of Bath**

## **Alternative formats**

If you require this document in an alternative format, please contact:  
[openaccess@bath.ac.uk](mailto:openaccess@bath.ac.uk)

### **General rights**

Copyright and moral rights for the publications made accessible in the public portal are retained by the authors and/or other copyright owners and it is a condition of accessing publications that users recognise and abide by the legal requirements associated with these rights.

### **Take down policy**

If you believe that this document breaches copyright please contact us providing details, and we will remove access to the work immediately and investigate your claim.

# Effect of particle size on the formation of $\text{Ti}_2\text{AlC}$ using combustion synthesis

T.Thomas<sup>1</sup> and C.R.Bowen

Materials and Structures Centre, Department of Mechanical Engineering, University of Bath, Bath, BA2 7AY, England, UK.

## Abstract

This paper provides an insight into the effect of particle size of elemental metal powders and carbon source on the formation mechanism of  $\text{Ti}_2\text{AlC}$  MAX-phase ceramic produced by self-propagating high-temperature synthesis (SHS). The effect of titanium, aluminium and carbon particle size on the  $2\text{Ti} + \text{Al} + \text{C} \rightarrow \text{Ti}_2\text{AlC}$  reaction, the phase evolution of the final product and the porosity in both the green body and product has been examined. The effect of the carbon source in the form of graphite, carbon black and short carbon fibres on the reaction mechanism is explained. It is found that the particle size of the titanium and aluminium reactants had little effect on the phases formed but affected the green density of the reactants and the porosity in the final product. The carbon source used in the combustion reaction had an influence on the phases formed by the SHS reaction and was influenced by the dispersion of carbon particles and the titanium-aluminium particle contact.

Keywords: SHS, Particle size, Porosity,  $\text{Ti}_2\text{AlC}$ , MAX-phase, XRD

---

<sup>1</sup> Materials and Structures Centre, Department of Mechanical Engineering, University of Bath, Bath, BA2 7AY, Email: tt295@bath.ac.uk

## 1. Introduction

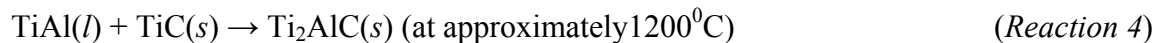
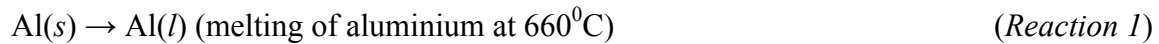
MAX-phase ceramics are a group of ductile ceramic materials with the molecular formula  $M_{n+1}AX_n$  ( $n = 1, 2, 3, \dots$ ), where M is an early transition element, A is an element from the 'A' group of the periodic table and X is either nitrogen or carbon [1]. A particular advantage of these materials is that they are able to maintain their strength at high temperatures. In addition these ceramic materials possess both ceramic and metallic properties; for example some of their important characteristics are low density, high stiffness, machinability, excellent thermal and electrical conductivity and the ability to exhibit a degree of plasticity at elevated temperature [2]. This fascinating combination of properties has led to researchers to consider the technological importance of these materials as a structural ceramic for high temperature applications.

One of the techniques to produce MAX-phase ceramics is by a solid-state combustion reaction also known as *self-propagating high temperature synthesis* (SHS) [3-6]. SHS is a technique developed for the production of engineering ceramics and other advanced materials [7]. The process involves the ignition of a compact powder reactant mixture in air or an inert atmosphere and an exothermic reaction produces sufficient heat that the reaction becomes self-sustaining; this results in the formation of combustion wave that propagates along the reactants to form the final desired product [8]. A variety of advanced materials, such as  $Ti_2AlC$ ,  $Ti_3AlC_2$ ,  $Ni_3Al$ ,  $Ni_2Al_3$ ,  $TiAl$ ,  $Zr_5Si_3$  [9], have been synthesised using this form of solid-state combustion synthesis reaction. The advantages of the SHS process are [7, 8] (i) the non-equilibrium behaviour of this process provides the opportunity to produce metastable phases due to the rapid rate of heating and relatively rapid cooling, (ii) the process is energy efficient compared to the traditional solid-state sintering process as the process takes place within few seconds depending on the exothermic nature of the reaction and the only necessary energy requirement is that to initiate the SHS reaction, (iii) the rapid exothermic reaction minimises the production time and (iv) due to the high temperature of the SHS reaction it is possible to produce products of high purity, since as any low boiling point impurities volatilise. However, the gases entrapped in the sample during the SHS reaction and the volume reduction during the reaction leads to the formation of a porous product [7]. However, this can be overcome by the application of external pressure to densify the product shortly after the SHS reaction has taken place [8].

SHS reactions are generally performed using a cold-pressed reactant powder mixture. As a result, the nature of the particle packing of the reactant mixture plays an important role in determining the green density, the thermal conductivity of the reactant mixture, the particle-particle contact and ultimately the microstructure, porosity and phases formed in the final product [10-16].

### 1.1 Formation mechanism of Ti<sub>2</sub>AlC

There are a variety of studies of the reaction mechanism to explain the evolution of the phases that are formed during combustion of Ti-Al-C based materials and SHS processing of Ti<sub>2</sub>AlC [17-19]. A number of reaction mechanisms focus on the temperature range associated with the formation of Ti<sub>2</sub>AlC and any intermediate compounds formed during the SHS process [18]. Other work [20] has examined the reaction pathway to form the final Ti<sub>2</sub>AlC product, which include Reactions 1-3 [18] and Reaction 4 [17];



Zhenbin et al. [19] refers to the mechanism as a solution-precipitation process as the TiC that is formed by Reaction 3 dissolves into the TiAl matrix formed by Reaction 2; this results in the precipitation of Ti<sub>2</sub>AlC by Reaction 4. Pietzka et al. [17] described the thermodynamics of the reaction mechanism and reported that the peritectic point of Ti<sub>2</sub>AlC is 1625±10°C and above this temperature Ti<sub>2</sub>AlC decomposes into TiC and Al. The Gibbs free energy, ΔG of Ti<sub>2</sub>AlC was found to decrease in magnitude with increasing temperature between 1000°C and 1300°C; where ΔG<sup>Ti<sub>2</sub>AlC</sup> (1000°C) = -65.9 kJ/mol and ΔG<sup>Ti<sub>2</sub>AlC</sup> (1300°C) = -54.8 kJ/mol. Therefore the optimum reaction temperature for forming the Ti<sub>2</sub>AlC phase may be at lower temperatures, e.g. 1000°C-1200°C. Hashimoto et al. and Liu et al. [21, 22] described mechanisms to explain the layered structure of these ternary carbides and how the reactant particle packing density influences the mechanism of formation of Ti<sub>2</sub>AlC by SHS. The thermodynamics and the adiabatic combustion temperature of the formation of Ti<sub>2</sub>AlC by SHS were considered by Bowen et al. in the form of enthalpy versus temperature curves [23].

## 1.2 Aims of paper

There are limited experimental studies explaining how the particle size of the metal reactants and variation of the particle size and nature of the carbon source plays an important role in reaction mechanism and this is the focus of this work. In this paper we report results from experiments conducted to understand the effect of particle size and carbon source during the formation of  $Ti_2AlC$  by a SHS reaction between the Ti, Al and C elemental reactants, as shown in Reaction 5.



The MAX-phase product,  $Ti_2AlC$ , belongs to Ti-Al-C [2] system and we will study how one can tune the porosity of the  $Ti_2AlC$  formed via SHS by changing the particle size of the elemental reactants and carbon source.

## 2. Experimental procedure

Elemental powders of titanium of different particle size included Ti-45 $\mu m$  (Goodfellow 99.5% purity) and Ti-25 $\mu m$  (Pi KEM Ltd, 99.9% purity). The aluminium particles size reactant were Al-15 $\mu m$ , Al-20  $\mu m$  and Al-60 $\mu m$  (Goodfellow 99.9% purity). The carbon sources used were short carbon fibres (mean diameter 3.55 $\mu m$ , mean length 104.14 $\mu m$ ), graphite  $\leq 20\mu m$  (Aldrich) and lamp black  $\leq 30\mu m$  (Inoxia Ltd).

To undertake the SHS reaction, each powder was mixed according to the stoichiometric molar ratio 2Ti:1Al:1C for 10 – 15 minutes using a mortar and pestle. The combination of above mentioned elements of various particle sizes were mixed to obtain the necessary reactant mixture for Reaction 5. A mass of 0.8g of the elemental powder mixture was pressed at room temperature into a compact cylindrical pellet of 13mm diameter in a uniaxial press using a pressure of 1.77kN/mm<sup>2</sup>. The thickness of the pellet varied with the different reactant particle sizes used, as seen in Table 1, and is related to degree of packing of the reactant. Field Emission Scanning Electron Microscopy (FESEM) images of the shape and size of the titanium, aluminium and carbon reactant particles are shown in figure 1.

**Table 1. Combination of particle sizes used and their green density. Sample diameter was 13mm and mass 0.8g in all cases. Note  $\text{Ti}_3\text{Al}$ ,  $\text{TiC}$  also formed when using Ti-25  $\mu\text{m}$ , Carbon fibre and Al of 15 $\mu\text{m}$  and 60 $\mu\text{m}$ .**

<b>Element, particle size (<math>\mu\text{m}</math>) and carbon source</b>	<b>Mean thickness (mm)</b>	<b>Green density (<math>\text{g}/\text{cm}^3</math>)</b>	<b>Compounds formed from SHS</b>
Ti-45, Al-15, Carbon fibre (mean diameter 3.55 $\mu\text{m}$ and length 105 $\mu\text{m}$ )	2.07	29.07	$\text{Ti}_2\text{AlC}$ , $\text{TiC}$
Ti-45, Al-25, Carbon fibre (mean diameter 3.55 $\mu\text{m}$ and length 105 $\mu\text{m}$ )	2.12	28.47	$\text{Ti}_2\text{AlC}$ , $\text{TiC}$
Ti-45, Al-60, Carbon fibre (mean diameter 3.55 $\mu\text{m}$ and length 105 $\mu\text{m}$ )	1.99	30.29	$\text{Ti}_2\text{AlC}$ , $\text{TiC}$
Ti-25, Al-15, Graphite $\leq 20\mu\text{m}$	1.79	33.61	$\text{Ti}_2\text{AlC}$ , $\text{TiC}$
Ti-25, Al-25, Graphite $\leq 20\mu\text{m}$	1.74	34.71	$\text{Ti}_2\text{AlC}$ , $\text{TiC}$
Ti-25, Al-60, Graphite $\leq 20\mu\text{m}$	1.78	33.92	$\text{Ti}_2\text{AlC}$ , $\text{TiC}$
Ti-45, Al-15, Graphite $\leq 20\mu\text{m}$	1.68	35.80	$\text{Ti}_2\text{AlC}$ , $\text{TiC}$
Ti-45, Al-25, Graphite $\leq 20\mu\text{m}$	1.71	35.18	$\text{Ti}_2\text{AlC}$ , $\text{TiC}$
Ti-45, Al-60, Graphite $\leq 20\mu\text{m}$	1.67	36.02	$\text{Ti}_2\text{AlC}$ , $\text{TiC}$
Ti-25, Al-15, Lamp black $\leq 30\mu\text{m}$	1.99	30.24	$\text{Ti}_2\text{AlC}$ , $\text{TiC}$
Ti-25, Al-25, Lamp black $\leq 30\mu\text{m}$	2.01	29.99	$\text{Ti}_2\text{AlC}$ , $\text{TiC}$
Ti-25, Al-60, Lamp black $\leq 30\mu\text{m}$	1.97	30.59	$\text{Ti}_2\text{AlC}$ , $\text{TiC}$
Ti-25, Al-25(0.3 mol excess), Carbon fibre (mean diameter 3.55 $\mu\text{m}$ and length 105 $\mu\text{m}$ )	2.08	29.02	???
Ti-25, Al-25, Carbon fibre (mean diameter 3.55 $\mu\text{m}$ and length 105 $\mu\text{m}$ )	2.14	28.12	$\text{Ti}_3\text{Al}$ , $\text{TiC}$

The cold pressed cylindrical pellets were loaded into a custom built combustion rig and ignited using a resistively heated ‘U’ shaped tungsten wire of 0.5mm diameter using 30A of electric current in an argon atmosphere at a pressure of 2 bar. The phases formed were analysed using XRD (using a Cu target) and the density and porosity of the SHS product was measured according to the BS EN623-2: 1993 standards.

### 3. Results and Discussion

Table 1 shows how the green density of the cold-pressed reactant pellets vary with the change in the particle size of the elemental powders indicating the porosity of the green body before the reaction process. The green density was measured since it provides an insight into the packing density of the 2Ti/Al/C reactants, since each pellet was mixed and cold-pressed under same conditions. The pellets were subjected to the SHS mode of combustion synthesis and the compounds detected from XRD for the respective combination of particle sizes are also provided in Table 1. The XRD analysis can be seen in figure 2 (graphite source), figure 3 (lamp black source) and figure 4 (carbon fibre source).

It can be observed that, irrespective of the particle size of both the titanium and aluminium, when graphite and lamp black was used as the carbon source, the final products were  $Ti_2AlC$  and  $TiC$ ; see Table 1 and the XRD results in figures 2 and 3. However, when carbon fibre was used the nature of the products formed is more complex (figure 4). As the particle size of the titanium decreases from  $45\mu m$  to  $25\mu m$ ,  $Ti_2AlC$  does not form, rather  $Ti_3Al$  is formed which is an intermediate compound formed during the formation of  $Ti_2AlC$ ; as explained by Ming et al. [18].

The cold-pressed pellets made with carbon fibre have the lowest green density compared to the reactant pellets formed using graphite and lamp black with similar particle size of titanium and aluminium; as seen in figure 5. The cold-pressed pellets made with carbon fibre (black colour bars in figure 5) have the lowest green density compared to the reactant pellets formed using both graphite and lamp black with Ti and Al of the same particle size. This is due to the relatively large size of the carbon fibre source compared to the titanium and aluminium, resulting in poor particle-particle contact that leads to an incomplete reaction between  $Ti_3Al$  and  $TiC$ , as seen in Table 1. In this case, only  $Ti_3Al$  is formed using carbon fibre source and the SHS reaction is not sustained for the formation of other intermediate compounds such as  $TiAl$  and  $TiC$ , which in turn reacts to form  $Ti_2AlC$ .

Figure 6 shows FESEM images showing how the reactant particles are packed when pressed into a green body. It can be seen that since the titanium, aluminium and carbon reactant particles are of different shape and size when mixed and pressed into pellets they form a variety of particle-particle interconnections depending on the relative particle size. For example, there is a point contact in the case of spherical particles (Figure 6e), line contact in the case of elongated particles (figure 6g) and multiple point contact when there is a large contrast between particle sizes (figure 6i). The nature of the powder packing also influence the appearance of the reactant pressed pellet, where the reactant mixtures with small carbon particles (graphite or lamp black) appear black to the naked eye since it coats the larger aluminium and titanium particles. Green body pellets formed with larger carbon fibres appear metallic in colour since the aluminium and titanium particles coat the larger carbon source. The nature of the packing also influences the green density of the cold pressed reactants, as seen in figure 5, which in turn can affect the SHS reaction process, the reactant thermal conductivity and therefore affect the propagation of the SHS combustion wave.

A possible reaction mechanism for pressed reactants made with titanium (25µm) and aluminium (15µm or 25µm) and short carbon fibre can be explained with the schematic in figure 7(a). When short carbon fibres are used as a carbon source, there is a greater degree of titanium to aluminium particle contact due to the shape and size of the carbon (figure 1(g) and figure 7(a)). As a result the green body pellet has a ‘metallic’ visual appearance due to poor dispersion of the short carbon fibres; this is shown by the particle arrangement representation in figure 7(a). When the cold pressed reactant is heated, due to high metal to metal contact, the thermal conductivity is high and as the combustion initiates and the propagating combustion wave moves across the reactants rapidly. This rapid propagation of combustion wave and poor dispersion of carbon particles, does not favour the completion of the final reaction step for the formation of  $Ti_2AlC$  via Reaction 4 but favours a reaction between titanium and aluminium:



and  $TiC$  by Reaction 3. The adiabatic combustion temperature of Reaction 6 is in excess of 1300°C [24]; and once complete there is relatively rapid cooling of the product after passage of the combustion wave since there is no reaction between  $TiAl$  and  $TiC$  to form  $Ti_2AlC$  via Reaction 4. As a result the XRD of the product formed by this composition indicates  $Ti_3Al$  and  $TiC$  (figure 4(ii)) as the main reaction product and the reactants pressed with 25µm titanium, 15µm or 25µm aluminium and short carbon fibre (figure 4(ii)) do not form  $Ti_2AlC$ .



However, when smaller graphite or lamp black particles are used as the carbon source, the carbon particles are in intimate contact with the titanium and aluminium particles due to the particle size and geometry; see figures 1(f) and 1(h). The particle arrangement is shown in the schematic in figure 7(b). As a result, the cold pressed reactants are both black in colour (this is in contrast to the green body reactant samples obtained using short carbon fibres, which appear metallic). In this case, there is a relatively poor titanium metal to aluminium metal contact as the carbon particles are located between the metal-metal reactant particles as seen in figure 7(b) and also the FESEM images in figures 6(a), (b), (c), (d), (e) and (j). This may also decrease the reactant thermal conductivity and slows down the propagating combustion wave as in figure 7(b). This leads to a slower propagation of combustion wave and ensures completion of Reactions 2, 3 and 4; thereby leading to the formation of  $Ti_2AlC$  by the solution precipitation mechanism [19] (Reaction 4). It is observed that in this case there is a slower ‘cooling down’ stage during the SHS reaction and the sample continues to ‘glow’ red after passage of the combustion wave due to progression of Reaction 4 to form  $Ti_2AlC$  after the combustion wave has passed, and this is more likely to occur in the case of reactant made with graphite and lamp black as seen in the schematic in figure 7(b).

To examine this hypothesis that a combustion wave associated with good particle-particle contact, a less exothermic reaction and slow cooling of the product after the combustion wave has passed favours the formation of  $Ti_2AlC$ , the aluminium content in the reaction mixture was increased in the reactant mixture made with short carbon fibres with  $25\mu m$  titanium and  $25\mu m$  aluminium. When excess Al ( $y$  in reaction 3) is added to the Reaction 1, it becomes:



The effect of diluents such as aluminium and titanium on the combustion reaction of  $Ti_2AlC$  was examined by Bowen et al. [23] and it was found that it decreases the exothermicity of the reaction, since the thermal mass of the system is increased. The addition of excess aluminium also served to increase the green density due to the presence of the ductile aluminium phase (see Table 1 and figure 5). Figure 8 is the XRD showing the evolution of compounds when a range of excess aluminium additions is used ( $y$  equivalent to 0.1, 0.2 and 0.3). When  $y=0.3$  the final product formed was  $Ti_2AlC$  (figure 8) and supports the theory that a higher green body density, higher carbon-metal particle contact and a lower combustion temperature leads to slow cooling of the sample upon the completion of the reaction and favours the formation of  $Ti_2AlC$  ceramic by SHS reaction.

Figure 9 shows the porosity of  $\text{Ti}_2\text{AlC}$  product formed with different combination of titanium, aluminium and carbon particle sizes; the porosity values are a mean of seven samples per reactant mixture. It can be observed that  $\text{Ti}_2\text{AlC}$  prepared with graphite is less porous than the other samples and is likely to be due to the higher green body density (see Figure 5) and the complete reaction to form the  $\text{Ti}_2\text{AlC}$ . The products formed using carbon fibres are more porous, again due to the lower initial density of the reactant (Figure 5) and incomplete reaction. This data is useful as it is a correlation to the exothermicity of the reaction and also aids in choosing the reactant particle size and carbon source for forming  $\text{Ti}_2\text{AlC}$  MAX-phase ceramics materials by SHS.

## 5. Conclusion

This paper has examined the influence of the particle size of the titanium, aluminium and carbon reactant on the products formed and thereby control phase evolution in  $\text{Ti}_2\text{AlC}$  MAX-phase ceramics manufactured by SHS. The particle size of the titanium and aluminium reactant has little effect on the final products formed. However, the shape and size of the carbon reactant particle has an influence on the packing density of the reactants and it was found that the more porous green body sample it is less likely to form  $\text{Ti}_2\text{AlC}$  and forms  $\text{Ti}_3\text{Al}$  and  $\text{TiC}$ , which is an intermediate compound, formed during the formation of  $\text{Ti}_2\text{AlC}$ . It was observed that high titanium-metal to aluminium-metal contact and large carbon particle size in the reactant pellet favours the formation of  $\text{Ti}_3\text{Al}$  and hinders the formation of  $\text{Ti}_2\text{AlC}$  by precipitation process. It was demonstrated that by lowering the combustion wave velocity by addition of diluents such as excess aluminium, it is possible to control the combustion wave and facilitate the formation of  $\text{Ti}_2\text{AlC}$ . It was also demonstrated that fine-tuning the carbon particle size could control the exothermicity of the reaction and control the porosity of the final product without the application of external pressure.

## Reference

- [1] M.W. Barsoum, The  $M_{N+1}AX_N$  phases: A new class of solids: Thermodynamically stable nano-laminates, *Progress in Solid State Chemistry*, 28 (2000) 201-281.
- [2] M.W. Barsoum, T. El-Raghy, The MAX Phases: Unique new carbide and nitride materials ternary ceramics turn out to be surprisingly soft and machinable, yet also heat-tolerant, strong and lightweight, *American Scientist*, 89 (2001) 334-343.
- [3] J.J. Berzelius, Beitrag zur näheren Kenntniss des Molybdän's, *Annalen der Physik*, 82 (1826) 331-350.
- [4] V. Hlavacek, Combustion synthesis: A historical perspective, *American Ceramic Society bulletin*, 70 (1991) 240-243.
- [5] J.W. McCauley, J.A. Puszynski, Historical perspective and contribution of US researchers into the field of self-propagating high-temperature synthesis (SHS)/combustion synthesis (CS): personal reflections, *International Journal of Self-propagating High-temperature Synthesis*, 17 (2008) 58-75.
- [6] J. Holt, Z. Munir, Combustion synthesis of titanium carbide: theory and experiment, *Journal of Materials Science*, 21 (1986) 251-259.
- [7] J.J. Moore, H. Feng, Combustion synthesis of advanced materials: Part I. Reaction parameters, *Progress in Materials Science*, 39 (1995) 243-273.
- [8] A. Varma, J.P. Lebrat, Combustion synthesis of advanced materials, *Chemical Engineering Science*, 47 (1992) 2179-2194.
- [9] A. Merzhanov, History and recent developments in SHS, *Ceramics International*, 21 (1995) 371-379.
- [10] S. Dubois, G.P. Bei, C. Tromas, C.V. Gauthier, P. Gadaud, Synthesis, microstructure, and mechanical properties of  $Ti_3Sn_{(1-x)}Al_xC_2$  MAX phase solid solutions, *International Journal of Applied Ceramic Technology*, 7 (2010) 719-729.
- [11] M. El Saeed, F.A. Deorsola, R. Rashad, Optimization of the  $Ti_3SiC_2$  MAX phase synthesis, *International Journal of Refractory Metals and Hard Materials*, 35 (2012) 127-131.
- [12] C. Hu, J. Zhang, J. Wang, F. Li, J. Wang, Y. Zhou, Crystal structure of  $V_4AlC_3$ : A new layered ternary carbide, *Journal of the American Ceramic Society*, 91 (2008) 636-639.
- [13] N.J. Lane, M. Naguib, J. Lu, L. Hultman, M.W. Barsoum, Structure of a new bulk  $Ti_5Al_2C_3$  MAX phase produced by the topotactic transformation of  $Ti_2AlC$ , *Journal of the European Ceramic Society*, 32 (2012) 3485-3491.
- [14] Y. Ming, Y. Chen, B. Mei, J. Zhu, Synthesis of high-purity  $Ti_2AlN$  ceramic by hot pressing, *Transactions of Nonferrous Metals Society of China*, 18 (2008) 82-85.

- [15] W.B. Tian, P.L. Wang, Y.M. Kan, G.J. Zhang, Y.X. Li, D.S. Yan, Phase formation sequence of  $\text{Cr}_2\text{AlC}$  ceramics starting from Cr–Al–C powders, *Materials Science and Engineering, A* 443 (2007) 229-234.
- [16] Y. Zhou, F. Meng, J. Zhang, New MAX-Phase Compounds in the V–Cr–Al–C System, *Journal of the American Ceramic Society*, 91 (2008) 1357-1360.
- [17] M. Pietzka, J. Schuster, Summary of constitutional data on the aluminium-carbon-titanium system, *Journal of Phase Equilibria*, 15 (1994) 392-400.
- [18] M. Bingchu, Y. Ming, Z. Jiaoqun, Z. Weibing, Preparation of  $\text{TiAl/Ti}_2\text{AlC}$  composites with Ti/Al/C powders by in-situ hot pressing, *Journal of Wuhan University of Technology-Materials Science Edition*, 21 (2006) 14-16.
- [19] Z. Ge, K. Chen, J. Guo, H. Zhou, J.M. Ferreira, Combustion synthesis of ternary carbide  $\text{Ti}_3\text{AlC}_2$  in Ti–Al–C system, *Journal of the European Ceramic Society*, 23 (2003) 567-574.
- [20] P. Wang, B. Mei, X. Hong, J. Zhu, W. Zhou, Fabrication of  $\text{Ti}_2\text{AlC}$  by spark plasma sintering from elemental powders and thermodynamics analysis of Ti–Al–C system, *Journal of Wuhan University of Technology-Materials Science Edition*, 22 (2007) 325-328.
- [21] S. Hashimoto, N. Nishina, K. Hirao, Y. Zhou, H. Hyuga, S. Honda, Y. Iwamoto, Formation mechanism of  $\text{Ti}_2\text{AlC}$  under the self-propagating high-temperature synthesis (SHS) mode, *Materials Research Bulletin*, 47 (2012) 1164-1168.
- [22] G. Liu, K. Chen, H. Zhou, J. Guo, K. Ren, J. Ferreira, Layered growth of  $\text{Ti}_2\text{AlC}$  and  $\text{Ti}_3\text{AlC}_2$  in combustion synthesis, *Materials Letters*, 61 (2007) 779-784.
- [23] T. Thomas, C.R. Bowen, Thermodynamic predictions for the manufacture of  $\text{Ti}_2\text{AlC}$  MAX-phase ceramic by combustion synthesis, *Journal of Alloys and Compounds*, 602 (2014) 72-77.
- [24] W.Y. Yang, G.C. Weatherly, A study of combustion synthesis of Ti–Al intermediate compounds, *Journal of Materials Science*, 31 (1996) 3707-3713.

## List of figures

Figure 1 FESEM images of the variety of titanium, aluminium and carbon particles used in this study:

(a) Al 15 $\mu$ m, (b) Al 25 $\mu$ m, (c) Al 60 $\mu$ m, (d) Ti 45 $\mu$ m, (e) Ti 25 $\mu$ m, (f) Lamp black  $\leq$ 30 $\mu$ m, (g) Carbon fibre and (h) Graphite  $\leq$ 20 $\mu$ m

Figure 2 XRD pattern (i) 45 $\mu$ m titanium (ii) 25 $\mu$ m titanium, with variety of size of aluminium particle sizes and graphite ( $\leq$ 20 $\mu$ m) as the carbon source

Figure 3 XRD pattern of the compounds formed when 25 $\mu$ m titanium is used with a variety of aluminium particle sizes and lamp black as the carbon source

Figure 4 XRD pattern (i) 45 $\mu$ m titanium (ii) 25 $\mu$ m titanium, with variety of size of aluminium particle sizes and carbon fibre as the carbon source

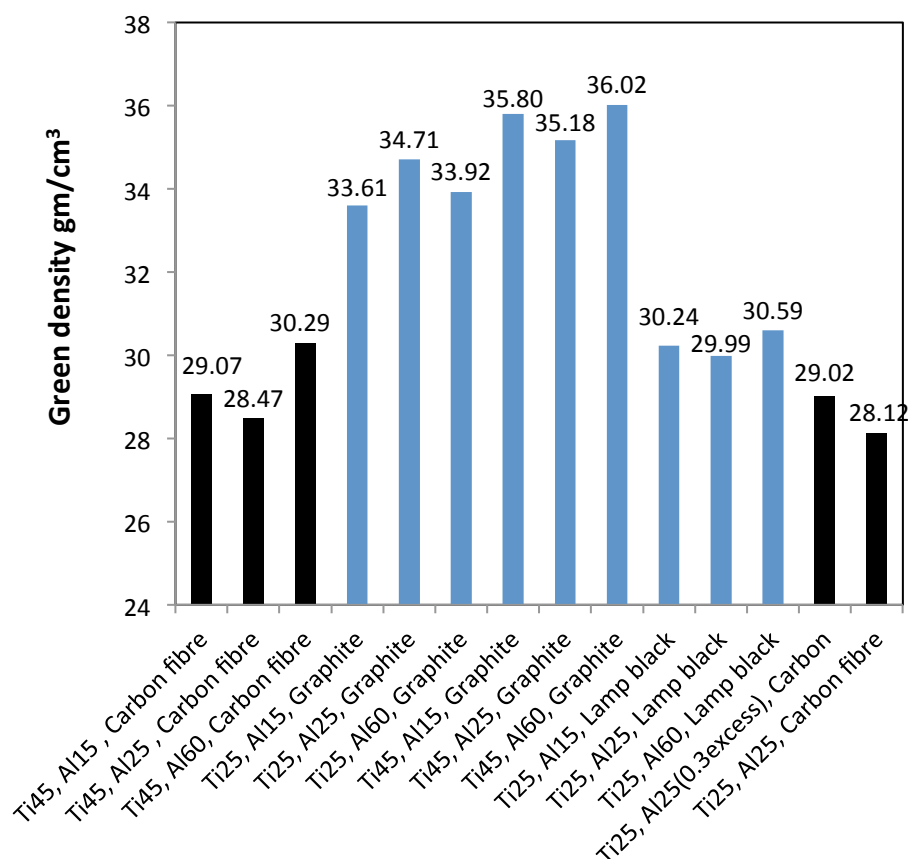


Figure 5 Green density of the cold pressed pellets pressed using various combinations of particle sizes

Figure 6 SEM images demonstrating packing of the reactant particles when cold pressed: (a) Ti 25 $\mu$ m, Al 15 $\mu$ m, Graphite, (b) Ti 25 $\mu$ m, Al 25 $\mu$ m, Graphite, (c) Ti 25 $\mu$ m, Al 60 $\mu$ m, Graphite, (d) Ti 45 $\mu$ m, Al 15 $\mu$ m, Graphite, (e) Ti 45 $\mu$ m, Al 25 $\mu$ m, Graphite, (f) Ti 45 $\mu$ m, Al 15 $\mu$ m, Carbon fibre, (g) Ti

45µm, Al 25µm, Carbon fibre, (h) Ti 25µm, Al 25µm, Carbon fibre, (i) Ti 25µm, (0.3 mol excess) Al 25µm, Carbon fibre, and (j) Ti 25µm, Al 25µm, Lamp black

Figure 7 (a) Schematic of the combustion process showing the effect of graphite/lamp black on the final product formed (a) Schematic showing the combustion reaction image showing the formation of  $Ti_2AlC$

Figure 8 XRD spectrum showing the evolution of compounds when excess Al is added to the reaction  $2Ti + (1 + y) Al + C \rightarrow Ti_2AlC + yAl$ . (a)  $y=0.1$ , (b)  $y=0.2$ , (c)  $y=0.3$

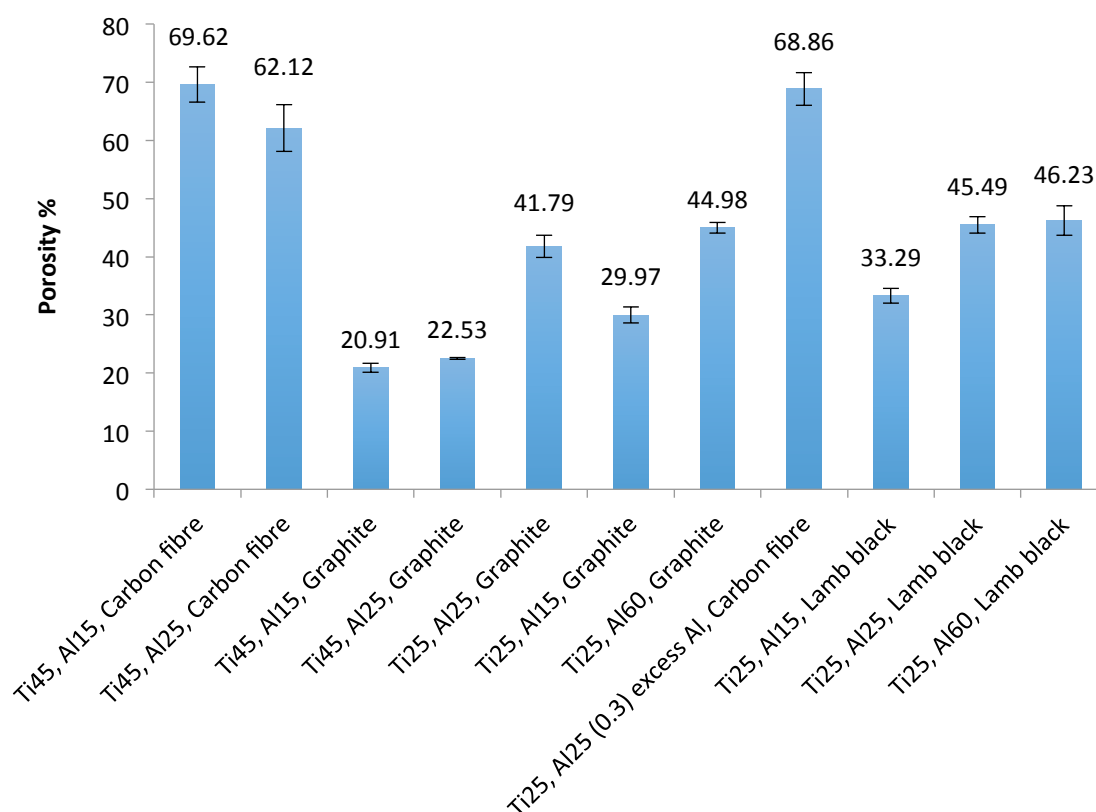


Figure 9 Porosity level (%) of the  $Ti_2AlC$  formed by SHS process from different combinations of particle sizes

